Low Pathogenicity Avian Influenza (H5N2) Viruses, Dominican Republic

David H. Chung, Dejelia R. Gomez, Julia M. Vargas, Belkis L. Amador, Mia K. Torchetti, Mary L. Killian, David E. Swayne, Dong-Hun Lee

Author affiliations: University of Connecticut, Storrs, Connecticut, USA (D.H. Chung, D.-H. Lee); Ministry of Agriculture, Roseau, Dominican Republic (D.R. Gomez, J.M. Vargas, B.L. Amador); US Department of Agriculture, Athens, Georgia, USA (D.E. Swayne); US Department of Agriculture, Ames, Iowa, USA (M.K. Torchetti, M.L. Killian)

DOI: https://doi.org/10.3201/eid2612.200268

Low pathogenicity avian influenza (H5N2) virus was detected in poultry in the Dominican Republic in 2007 and re-emerged in 2017. Whole-genome sequencing and phylogenetic analysis show introduction of an H5N2 virus lineage from Mexico into poultry in the Dominican Republic, then divergence into 3 distinct genetic subgroups during 2007–2019.

Low pathogenicity avian influenza virus (LPAIV) subtype H5N2 has caused outbreaks in poultry in Mexico since 1993 and mutated into highly pathogenic avian influenza virus (HPAIV) H5N2 during 1994–1995 (*1*). In 1994, a vaccination program against H5N2 in poultry was established in Mexico; HPAIV H5N2 was eradicated there in 1995 (*2*). However, LPAIV H5N2 persisted and related viruses spread to neighboring countries (*1*,*3*,*4*). In addition, the H5N2 virus lineage from Mexico was introduced to Taiwan in 2003, likely because of inadequately inactivated vaccines. The virus then reassorted with the local avian influenza (H6N1) virus strain that has been enzootic in chickens in Taiwan since 1997 to produce reassortant H5N2 virus possessing hemagglutinin (HA) and neuraminidase (NA) genes of H5N2 virus from Mexico and internal genes of the Taiwan H6N1 virus. The reassortant H5N2 virus mutated into an HPAIV and caused outbreaks in poultry in Taiwan during 2012 (*5*).

In 2007, outbreaks of LPAIV H5N2 occurred among chickens in Santo Domingo and Higüey-La Otra Banda, Dominican Republic, and were reported to the World Organisation for Animal Health (OIE) (*6*). The OIE Reference Laboratory detected LPAIV H5N2 lineages from Mexico in samples from the Dominican Republic outbreaks on December 21, 2007. During December 2007–February 2008, a total of 11 avian influenza A viruses were detected in the Dominican Republic from backyard birds, fighting birds, and a live bird market (*7*) (Appendix Table 1, https://wwwnc.cdc.gov/EID/article/26/12/20-0268-App1.pdf). During 2007–2016, serologic surveillance of poultry detected 364/45,440 (0.80%) samples exhibiting positive antibody responses, suggesting low level circulation of LPAIVs in the Dominican Republic, but the HA and NA subtypes were not identified (data not shown). During September–November 2017, the H5N2 LPAIV re-emerged and affected 5 commercial chicken farms in Espaillat, San Juan, and La Vega (Appendix Table 2). Subsequently, the viruses were detected in 23 commercial and backyard poultry flocks during September 2018–February 2019 (*8*). During the 2017–2019 H5N2 LPAIV outbreak period, seropositivity reached 52% (8,740/16,543).

Since 2007, limited information on H5N2 LPAIVs and few genetic sequences have been reported. We provide sequenced genomes of 19 H5N2 LPAIVs identified in the Dominican Republic during 2007–2019: 1 virus from 2007, 6 from 2017, 1 from 2018, and 11 from 2019.

The 2007 H5N2 LPAIV, Ck/Dominican_Republic/2007(H5N2), had an HA cleavage site sequence with 2 basic amino acids (PQRETR/G). However, the 2017–2019 viruses possessed 3 monobasic amino acids (PQRGKR/G, PQREKR/G, and LQREKR/G) (Appendix Table 3). Seven representative isolates were of low pathogenicity in chickens on intravenous inoculation (intravenous pathogenicity index = 0.0). The acquisition of an additional basic amino acid in the HA cleavage site raises a concern regarding the increased risk for mutation to an HPAIV.

All genes formed a well-supported monophyletic clade (bootstrap support of 98–100 in maximum likelihood phylogeny and posterior probability of 0.99–1.00 in Bayesian phylogeny), suggesting their close relationship from a single viral introduction into the poultry population descended from A/Ck/Hidalgo/28159–232/94 (H5N2)–like virus and maintenance in poultry in the Dominican Republic (Figure 1; Appendix Figures 1–8). The inferred time to most recent common ancestor (tMRCA) for each gene of H5N2 viruses identified in the Dominican Republic ranged from February 2005 to August 2006, suggesting that ancestors of these viruses emerged from an H5N2 virus lineage introduced from Mexico during this period (Appendix Table 4). Phylogenetic analyses show divergence of all 8 gene segments into 3 genetic sublineages

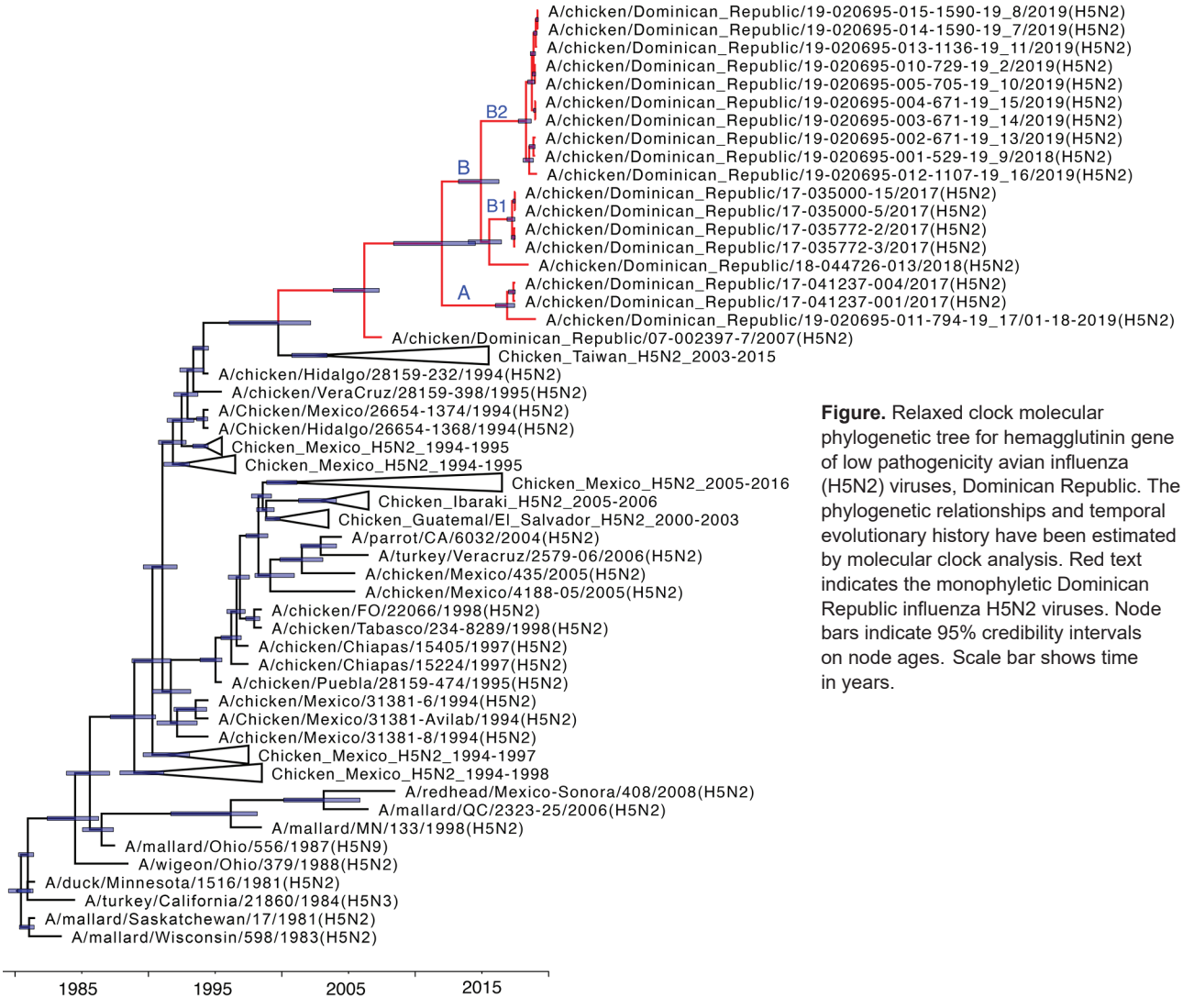

Figure. Relaxed clock molecular phylogenetic tree for hemagglutinin gene of low pathogenicity avian influenza (H5N2) viruses, Dominican Republic. The phylogenetic relationships and temporal evolutionary history have been estimated by molecular clock analysis. Red text indicates the monophyletic Dominican Republic influenza H5N2 viruses. Node bars indicate 95% credibility intervals on node ages. Scale bar shows time in years.

designated as sublineage A, which contains viruses collected in 2017 and 2019; B1, which contains viruses collected during 2017; and B2, which contains viruses collected during 2018–2019. The 8 gene segments of Ck/Dominican_Republic/044726_013/2018(H5N2) fell into sublineage B (Appendix Table 3).

The prediction of N-linked glycosylation sites in the HA protein revealed that the H5N2 LPAIVs have 9 potential glycosylation sites at position 27, 39, 142, 181, 252, 277, 302, 496, and 555 (H5 numbering system), with a range of 6–8 sites for individual isolates (Appendix Table 5, Figure 9). The potential glycosylation at positions 142, 181, and 252 were found within antigenic sites (*9*). The initially identified Ck/Dominican_Republic/2007(H5N2) was predicted to contain N-linked glycosylation at the antigenic sites at positions 181 and 252. Sublineage A and B1 did not have the predicted glycosylation at position 252 but gained additional glycosylation at position 142. However, sublineage B2 was predicted to possess glycosylation at all antigenic sites at positions 142, 181, and 252, except for the Ck/Dominican_Republic/020695-012-1107-19-16/2019 (H5N2) strain, which has N-glycosylation only at positions 142 and 252.

Enhanced active surveillance is required to monitor the evolution and spread of H5N2 viruses in the Dominican Republic; such efforts could further the epidemiologic understanding and the design of improved prevention strategies. Additional studies could elucidate whether the genetic changes in glycosylation and antigenic sites contribute to the alterations in antigenicity of the H5N2 LPAIV from the Dominican Republic against current H5 virus vaccine strains.

Acknowledgment

We thank Julia Desiato for technical assistance.

D.-H.L. and D.H.C. are partially supported by the US Department of Agriculture, Agricultural Research Service project no. 6040-32000-066-51S.

About the Author

Mr. Chung is a PhD student at the University of Connecticut, Storrs, Connecticut, USA. His primary research interests include the molecular epidemiology of avian influenza and other zoonotic viruses.

References

1. Villarreal-Chávez C, Rivera-Cruz E. An update on avian influenza in Mexico. Avian Dis. 2003;47(Suppl):1002–5. https://doi.org/10.1637/0005-2086-47.s3.1002
2. Escorcia M, Vázquez L, Méndez ST, Rodríguez-Ropón A, Lucio E, Nava GM. Avian influenza: genetic evolution under vaccination pressure. Virol J. 2008;5:15. https://doi.org/10.1186/1743-422X-5-15
3. Abdelwhab SM, Veits J, Mettenleiter TC. Genetic changes that accompanied shifts of low pathogenic avian influenza viruses toward higher pathogenicity in poultry. Virulence. 2013;4:441–52. https://doi.org/10.4161/viru.25710
4. Bublot M, Pritchard N, Swayne DE, Selleck P, Karaca K, Suarez DL, et al. Development and use of fowlpox vectored vaccines for avian influenza. Ann N Y Acad Sci. 2006;1081:193–201. https://doi.org/10.1196/annals.1373.023
5. Lee CC, Zhu H, Huang PY, Peng L, Chang YC, Yip CH, et al. Emergence and evolution of avian H5N2 influenza viruses in chickens in Taiwan. J Virol. 2014;88:5677–86. https://doi.org/10.1128/JVI.00139-14
6. World Organization for Animal Health. Report on low pathogenic avian influenza virus in Dominican Republic, H5N2 2007. 2007 Dec 21 [cited 2019 Dec 10]. https://www.oie.int/wahis_2/public/wahid.php/Reviewreport/Review?page_refer=MapEventSummary&reportid=6616
7. World Organization for Animal Health. Report on low pathogenic avian influenza virus in Dominican Republic, H5N2 2009. 2009 Aug 21 [cited 2019 Dec 10]. https://www.oie.int/wahis_2/public/wahid.php/Reviewreport/Review?reportid=6882
8. World Organization for Animal Health. Report on low pathogenic avian influenza virus in Dominican Republic, H5N2 2019. 2019 Oct 16 [cited 2019 Dec 10]. https://www.oie.int/wahis_2/public/wahid.php/Reviewreport/Review?reportid=31880
9. Kaverin NV, Rudneva IA, Govorkova EA, Timofeeva TA, Shilov AA, Kochergin-Nikitsky KS, et al. Epitope mapping of the hemagglutinin molecule of a highly pathogenic H5N1 influenza virus by using monoclonal antibodies. J Virol. 2007;81:12911–7. https://doi.org/10.1128/JVI.01522-07

Address for correspondence: Dong-Hun Lee, Department of Pathobiology & Veterinary Science, University of Connecticut, 61 N Eagleville Rd, Unit-3089, Storrs, CT 06269, USA; email: dong-hun.lee@uconn.edu

Autochthonous Ratborne Seoul Virus Infection in Woman with Acute Kidney Injury

Jörg Hofmann,[1] Elisa Heuser,[1] Sabrina Weiss,[2] Beate Tenner, Konrad Schoppmeyer, Jutta Esser, Christiane Klier, Stephan Drewes, Rainer G. Ulrich, Detlev H. Kruger

Author affiliations: Charité–Universitätsmedizin Berlin, Berlin, Germany (J. Hofmann, S. Weiss, B. Tenner, D.H. Kruger); Friedrich-Loeffler-Institut, Greifswald-Insel Riems, Germany (E. Heuser, S. Drewes, R.G. Ulrich); Euregio-Klinik, Medizinische Klinik II, Nordhorn, Germany (K. Schoppmeyer); Laborarztpraxis Osnabrück, Georgsmarienhütte, Germany (J. Esser); German Center for Infection Research, Partner Site Hamburg-Lübeck-Borstel-Insel Riems, Germany (E. Heuser, R.G. Ulrich); Public Health Agency of Lower Saxony, Hannover, Germany (C. Klier)

DOI: https://doi.org/10.3201/eid2612.200708

Outside Asia, Seoul virus (SEOV) is an underestimated pathogen. In Germany, autochthonous SEOV-associated hantavirus disease has not been unequivocally diagnosed. We found clinical and molecular evidence for SEOV infection in a young woman; her pet rat was the source of infection.

Hantavirus infections cause febrile and often life-threatening zoonoses known as hemorrhagic fever with renal syndrome and hantavirus cardiopulmonary syndrome. Human pathogenic hantavirus species usually are carried by specific rodent reservoirs, which shed infectious virus in their excreta (*1*).

Seoul virus (SEOV), a species within the genus *Orthohantavirus*, is hosted by Norway or brown rats (*Rattus norvegicus*) and other *Rattus* species as main reservoir. SEOV-associated hantavirus disease is characterized by fever, acute kidney injury, often hepatitis and gastroenteritis, associated with transient thrombocytopenia and proteinuria (*2*,*3*). Most clinical cases are known to originate from China and South Korea; however, SEOV infection can occur worldwide because of the global distribution of Norway rats in the wild. Moreover, human infection has been described from contact with breeder rats (laboratory rats and laboratory rat–derived tissue cultures), pet rats, and feeder rats (*3*–*6*).

SEOV-caused hantavirus disease, especially in areas outside Asia to which it is not endemic, is

[1]These authors contributed equally to this article.

[2]Current affiliation: Robert Koch Institute, Berlin, Germany.

Article DOI: https://doi.org/10.3201/eid2612.200268

Mexican-Lineage Low Pathogenicity Avian Influenza (H5N2) Viruses, Dominican Republic

Appendix

Materials and Methods

We sequenced complete genomes of 19 low pathogenicity avian influenza viruses (LPAIVs) identified in the Dominican Republic during 2007–2019, including 1 from 2007, 6 from 2017, 1 from 2018, and 11 from 2019. We extracted viral RNA by using the MagMAX Viral RNA Isolation Kit (Ambion/ThermoFisher Scientific, https://www.thermofisher.com). All 8 segments of isolates were amplified by multi-segment reverse transcription-PCR (*1*) and whole-genome sequencing was conducted by using the Miseq system (Illumina, https://www.illumina.com). We used the Nextera XT DNA Sample Preparation Kit (Illumina) to generate multiplexed paired-end sequencing libraries, according to the manufacturer's instructions. The dsDNA was fragmented and tagged with adapters by Nextera XT transposase and 12-cycle PCR amplification. Fragments were purified on Agencourt AMpure XP beads (Beckman Coulter, https://www.beckmancoulter.com) and analyzed on a High Sensitivity DNA Chip on the Bioanalyzer (Agilent Technologies, https://www.agilent.com). The barcoded multiplexed library sequencing was performed by using the 250 cycle MiSeq Reagent Kit v2 (Illumina). We performed de novo and directed assembly of genome sequences by using SeqMan NGen version 4 (https://www.nihlibrary.nih.gov/resources/tools/seqman-ngen). We deposited nucleotide sequences in GenBank (Appendix Table 3).

For phylogenetic analysis, we downloaded all sequences of H5N2 virus lineages from Mexico were downloaded from the National Center for Biotechnology Information Influenza Virus Resource database (https://www.ncbi.nlm.nih.gov) and added to sequence alignments in September 2019. On the basis of BLAST (http://blast.ncbi.nlm.nih.gov/Blast.cgi) searches of HA and NA genes, North American lineage avian influenza virus sequences that were collected

before the emergence of H5N2 lineage from Mexico were added. Multiple sequence alignments were prepared using Multiple Alignment with Fast Fourier Transformation (MAFFT; https://mafft.cbrc.jp), and manual optimization of the alignment was done by using BioEdit (https://bioedit.org) to trim nucleotide positions to only use protein coding regions for phylogenetic analyses using 70 sequences each for polymerase (PA), polymerase basic 2 [PB2] , PB1, and matrix (M) segments; 71 sequences for nonstructural protein (NSP); 73 sequences for neuraminidase (NA) segment; 180 hemagglutinin (HA) segment; and 68 sequences for nucleoprotein (NP) segment. Maximum-likelihood (ML) phylogenies of each gene segment were estimated with RAxML program (*2*) using the GTR model of nucleotide substitution with gamma-distributed site heterogeneity rate variation. Bootstrap analysis was conducted via rapid bootstrap with 1,000 replicates for statistical support of generated tree topology.

The Bayesian relaxed clock phylogenetic analysis of the 8 segments was performed by using BEAST version 1.10.4 (*3*). TempEst software (https://www.beast.community/tempest) was used to investigate suitable correlation of the temporal signal and clock-likeness of phylogenies for phylogenetic molecular clock BEAST analysis based on collection date and genetic divergence (*4*). We applied an uncorrelated lognormal distribution relaxed clock method, the Hasegawa-Kishino-Yano (HKY) nucleotide substitution model with 4 categories and the Gaussian Markov random field (GMRF) Bayesian skyride coalescent prior (*5*). We ran a Markov chain Monte Carlo (MCMC) method to sample trees and ran evolutionary parameters for 5.0×10^7 generations for HA gene and 3.0×10^7 generations for the other 7 genes. We combined ≥ 3 independent chains to ensure adequate sampling of the posterior distribution of trees. We used TRACER version 1.7.1 (http://beast.community/tracer) with 10% burn-in to confirm convergence of each BEAST output and sufficient effective sample size (>200). We generated a maximum clade credibility (MCC) tree for each dataset by using TreeAnnotator in BEAST. We used FigTree 1.4.4 (http://tree.bio.ed.ac.uk) for visualization of MCC trees and estimated the time to the most recent common ancestor (tMRCA) of each clade.

We predicted potential N-glycosylation sites by using NetNGlyc server 1.0 (http://www.cbs.dtu.dk/services/NetNGlyc) and GlyProt (http://www.glycosciences.de/modeling). We modeled the HA structure by using the previously published 3-dimensional (3D) structure (PDB ID: 5ykc) in the SWISS-MODEL server (https://swissmodel.expasy.org). We created visualizations of 3D HA structures by using the

PyMOL Molecular Graphics System Version 2.0 (Schrödinger, LLC, https://www.schrodinger.com).

For the intravenous pathogenicity index of viruses, 10 6-week-old specific pathogen free chickens were inoculated intravenously with 0.1 ml of 1:10 dilutions of infectious allantoic fluids. The intravenous pathogenicity index (IVPI) was calculated according to the World Organization for Animal Health standard protocol (http://www.oie.int/international-standard-setting/terrestrial-code). Isolates with an IVPI >1.2 were determined to be HPAI. The challenge study and all experiments with live viruses were conducted in a Biosafety Level 3 facility.

References

1. Chrzastek K, Lee DH, Smith D, Sharma P, Suarez DL, Pantin-Jackwood M, et al. Use of Sequence-Independent, Single-Primer-Amplification (SISPA) for rapid detection, identification, and characterization of avian RNA viruses. Virology. 2017;509:159–66. PubMed https://doi.org/10.1016/j.virol.2017.06.019

2. Stamatakis A. RAxML version 8: a tool for phylogenetic analysis and post-analysis of large phylogenies. Bioinformatics. 2014;30:1312–3. PubMed https://doi.org/10.1093/bioinformatics/btu033

3. Drummond AJ, Rambaut A. BEAST: Bayesian evolutionary analysis by sampling trees. BMC Evol Biol. 2007;7:214. PubMed https://doi.org/10.1186/1471-2148-7-214

4. Rambaut A, Lam TT, Max Carvalho L, Pybus OG. Exploring the temporal structure of heterochronous sequences using TempEst (formerly Path-O-Gen). Virus Evol. 2016;2:vew007. PubMed https://doi.org/10.1093/ve/vew007

5. Minin VN, Bloomquist EW, Suchard MA. Smooth skyride through a rough skyline: Bayesian coalescent-based inference of population dynamics. Mol Biol Evol. 2008;25:1459–71. PubMed https://doi.org/10.1093/molbev/msn090

Appendix Table 1. Summary of World Organization for Animal Health report on Mexican-lineage low pathogenicity avian influenza H5N2 virus outbreak, Dominican Republic, December 2017–February 2018

No.	Date	Region	Unit	No. susceptible	No. cases	No. deaths	No. killed and disposed	No. slaughtered	Affected population
1	2007 Dec 12	Higuey, La Otra Banda, La Altagracia	Village	15	1	0	0	15	–
2	2007 Dec 12	Traspatio, Santo Domingo, Distrito Nacional	Village	115	1	0	0	115	Live bird market
3	2007 Dec 21	San Pedro de Macoris, San Pedro de Macoris, San Pedro De Macoris	Village	5	1	0	5	0	–
4	2008 Jan 4	La Vega, Bacuí, Barranca, La Vega	Village	26	1	0	26	0	Fighting cock from Higuey
5	2008 Jan 10	Villa El Sombrero, El Sombrero, Baní, Peravia	Village	114	1	0	114	0	–
6	2008 Jan 11	La Otra Banda, Cruce del Isleño, La Otra Banda, La Altagracia	Village	330	0	0	0	330	Fighting birds
7	2008 Jan 16	Santo Domingo Oeste, Hato Nuevo, Santo Domingo, Distrito Nacional	Village	205	1	0	205	–	Fighting cocks
8	2008 Jan 18	Batey Central, Barahona	Village	30	0	0	0	30	Fighting cocks
9	2008 Jan 26	Corbano Sur, San Juan	Village	5	0	0	0	5	Backyard birds
10	2008 Jan 28	Villa Gonzalez, La Delgada, Villa Gonzalez, Santiago	Village	22	0	0	0	22	Fighting cocks
11	2008 Feb 4	Pedernales, Pedernales	Village	4	0	0	0	4	Fighting cocks
Total	–	–	–	871	6	0	350	521	–

Statistics	Apparent morbidity rate, %	Apparent mortality rate, %	Apparent case fatality rate, %	Proportion susceptible animals lost, %
	0.69	0.00	0.00	100.00

Appendix Table 2. Summary of World Organization for Animal Health report on Mexican-lineage low pathogenicity avian influenza H5N2 virus outbreaks, Dominican Republic, September 2017–June 2019

No.	Date	Region	Epidemiology Unit	No. susceptible	No. cases	No. deaths	No. killed and disposed	No. slaughtered	Affected population
12	2017 Sep 30	Espaillat, Guanabano, Moca, Espaillat	Farm	48,877	1,953	1,953	46,924	0	Population kept in a farm composed of 8 layer units
13	2017 Oct 10	San Juan, Sabana Alta, San Juan de la Maguana, San Juan	Farm	46,500	12,657	12,657	33,843	0	Broiler chickens in 3 sheds
14	2017 Oct 10	La Vega, Río Verde Arriba, Arroyo Hondo, Rio Verde Arriba, La Vega	Farm	34,000	1,639	1,639	32,361	0	Layer hens in 5 sheds
15	2017 Oct 30	La Vega, Cutupú, Río Verde Arriba, La Vega	Farm	27,410	1,257	1,257	26,153	0	Layer hens in 4 sheds
16	2017 Dec 11	La Vega, Cutupú, Cutupú, Rio Verde Arriba, La Vega	Farm	35,000	43	43	34,957	0	Layer hens in production
17	2018 Jan 9	Salcedo/Hermanas Mirabal, Jayabo, Salcedo, Salcedo	Farm	11,500	785	785	10,715	0	Layer hens in 2 sheds
18	2018 Jan 9	Salcedo/Hermanas Mirabal, Jayabo, Salcedo, Salcedo	Farm	32,400	–	0	32,400	0	Layer hens in production
19	2018 Jan 10	La Vega, Rio Verde Arriba, Arroyo Hondo, Rio Verde Arriba, La Vega	Farm	26	6	0	26	0	Backyard hens
20	2018 Mar 20	La Vega, Río Verde Arriba, Cutupú, Rio Verde Arriba, La Vega	Farm	34,500	30	30	34,470	0	Layer hens distributed between 3 coops
21	2018 Apr 2	La Vega, Caguey, Rio Verde Arriba, La Vega	Farm	22,965	46	46	22,919	0	Layer hens distributed between 4 coops
22	2018 Nov 2	Puerto Plata, Cayacoa, Luperón, Puerto Plata	Backyard	1,126	773	745	136	217	Backyard birds (hens, ducks, turkeys and guinea fowls)
23	2018 Dec 30	Espaillat, El Corozo, Moca, Espaillat	Farm	1,800	30	–	0	0	Family farm with Israeli chicks
24	2018 Dec 27	Puerto Plata, Cayacoa, Luperón, Puerto Plata	Backyard	55	7	7	48	0	Laying hens
25	2019 Jan 8	Espaillat, Quebrada Honda, Moca, Espaillat	Backyard	56,685	2,350	2,350	0	54,335	Family farm with heavy birds
26	2019 Jan 8	Espaillat, El Corozo, Moca, Espaillat	Farm	3,000	27	–	0	0	Family farm with Israeli chicks
27	2019 Jan 10	Espaillat, El Caminito de la Rosario, Moca, Espaillat	Farm	45,000	535	530	0	0	Light layer birds
28	2019 Jan 14	Espaillat, Hincha, Moca, Espaillat	Farm	18,000	10	–	0	17,990	Light layer birds
29	2019 Jan 21	Espaillat, Las Lagunas, Moca, Espaillat	Farm	59,097	21	–	0	0	Backyard poultry
30	2019 Jan 22	Espaillat, Monte de la Jagua, Moca, Espaillat	Backyard	19	12	7	0	0	Backyard poultry

No.	Date	Region	Epidemiology Unit	No. susceptible	No. cases	No. deaths	No. killed and disposed	No. slaughtered	Affected population
31	2019 Jan 24	Santo Domingo, Mal Nombre, La Victoria, Distrito Nacional	Backyard	50	30	–	0	0	Fighting cocks
32	2019 Feb 5	Espaillat, Juan López, Moca, Espaillat	Farm	14,170	2,330	2,330	0	10,050	Broilers
33	2019 Feb 5	Espaillat, Cuero Duro, San Victor, Espaillat	Farm	3,500	550	550	0	2,950	Broilers
34	2019 Feb 10	Salcedo, La ceiba, Villa Tapa, Salcedo	Farm	96,963	9	6	0	0	Light layers
35	2019 Feb 21	La Vega, Monte Adentro, La Vega, La Vega	Farm	3,500	10	5	0	3,490	Light layers
36	2019 Feb 23	San José de Ocoa, El Estrecho, Rancho Arriba, San Jose De Ocoa	Farm	45,000	7,145	2,140	37,855	0	Heavy layers
37	2019 May 8	Santiago, Tamboril, Tamboril, Santiago	Farm	247,718	5	–	0	247,713	Broilers
38	2019 May 22	La Vega, Rio Verde, La Vega, La Vega	Farm	19,500	1	–	0	0	Light layers
39	2019 Jun 2	Espaillat, Las Barias, Moca, Espaillat	Farm	25,000	11	–	0	24,989	Israeli-bred hens
Total	–	–	–	933,361	32,272	27,080	312,807	361,734	–

Statistics	Apparent morbidity rate, %	Apparent mortality rate, %	Apparent case fatality rate, %	Proportion susceptible animals lost, %
	3.46	2.90	83.91	75.17

Appendix Table 3. Strain, collection date, and GenBank accession numbers for low pathogenicity avian influenza H5N2 viruses used in this study

Strain	Collection date	Accession no.	Segments (sublineages)								HA cleavage site motif	IVPI
			PB2	PB1	PA	HA	NP	NA	M	NS		
A/CK/DR/07_002397_7/2007	2007	MN882390–7	–	–	–	–	–	–	–	–	PQRETR/G	0
A/CK/DR/17_041237_001/2017	2017	MN882430–37	A	A	A	A	A	A	A	A	PQRGKR/G	0
A/CK/DR/17_035772_2/2017	2017	MN882414–21	B1	B1	B1	B1	B1	B1	B1	B1	PQREKR/G	ND
A/CK/DR/17_035772_3/2017	2017	MN882422–29	B1	B1	B1	B1	B1	B1	B1	B1	PQREKR/G	ND
A/CK/DR/17_035000_5/2017	2017	MN882398–405	B1	B1	B1	B1	B1	B1	B1	B1	PQREKR/G	0
A/CK/DR/17_035000_15/2017	2017	MN882406–13	B1	B1	B1	B1	B1	B1	B1	B1	PQREKR/G	0
A/CK/DR/17_041237_004/2017	2017	MN882438–45	A	A	A	A	A	A	A	A	PQRGKR/G	ND
A/CK/DR/18_044726_013/2018	2018	MN882446–53	B	B	B	B	B	B	B	B	PQREKR/G	0
A/CK/DR/18_020695_001_529_19_9/2018	2018 Dec 13	MN882454–61	B2	B2	B2	B2	B2	B2	B2	B2	LQREKR/G	0
A/CK/DR/19_020695_002_671_19_13/2019	2019 Jan 9	MN882462–69	B2	B2	B2	B2	B2	B2	B2	B2	LQREKR/G	ND
A/CK/DR/19_020695_003_671_19_14/2019	2019 Jan 9	MN882470–77	B2	B2	B2	B2	B2	B2	B2	B2	LQREKR/G	ND
A/CK/DR/19_020695_004_671_19_15/2019	2019 Jan 9	MN882478–85	B2	B2	B2	B2	B2	B2	B2	B2	LQREKR/G	ND
A/CK/DR/19_020695_005_705_19_10/2019	2019 Jan 11	MN882486–93	B2	B2	B2	B2	B2	B2	B2	B2	LQREKR/G	ND
A/CK/DR/19_020695_010_729_19_2/2019	2019 Jan 15	MN882494–501	B2	B2	B2	B2	B2	B2	B2	B2	LQREKR/G	ND
A/CK/DR/19_020695_011_794_19_17/2019	2019 Jan 18	MN882502–509	A	A	A	A	A	A	A	A	LQREKR/G	0
A/CK/DR/19_020695_012_1107_19_16/2019	2019 Feb 18	MN882510–517	B2	B2	B2	B2	B2	B2	B2	B2	PQRGKR/G	ND
A/CK/DR/19_020695_013_1136_19_11/2019	2019 Feb 18	MN882518–525	B2	B2	B2	B2	B2	B2	B2	B2	LQREKR/G	ND
A/CK/DR/19_020695_014_1590_19_7/2019	2019 Mar 25	MN882526–533	B2	B2	B2	B2	B2	B2	B2	B2	LQREKR/G	ND
A/CK/DR/19_020695_015_1590_19_8/2019	2019 Mar 25	MN882534–541	B2	B2	B2	B2	B2	B2	B2	B2	LQREKR/G	ND

*CK, chicken, DR, Dominican Republic; IVPI, intravenous pathogenicity index; ND, not done; –, initially detected H5N2 virus in Dominican Republic.

Appendix Table 4. Estimated time to the most recent common ancestor (tMRCA) for each gene segment isolated with 95% highest posterior density, Dominican Republic

Segment	tMRCA	95% HPD interval		Posterior
		Begin	End	
PB2	2006 Aug 29	2004 Jan 3	2007 Jul 2	1
PB1	2006 Aug 6	2002 Jan 18	2007 Jul 2	0.99
PA	2005 Jun 22	2002 Mar 12	2007 Apr 16	1
HA	2006 Mar 8	2003 Nov 8	2007 Apr 17	0.99
NP	2005 Feb 27	2001 May 8	2007 May 11	1
NA	2006 Mar 4	2003 Aug 8	2007 Jun 7	1
M	2006 Mar 9	2003 May 19	2007 Jun 2	1
NS	2005 May 1	2001 Jan 5	2007 Mar 6	1

*tMRCA were calculated by using bayesian evolutionary analysis sampling trees (BEAST). HPD, highest posterior density; PB2, polymerase basic 2; PB1, polymerase basic 1; PA, polymerase acidic; HA, hemagglutinin; NP, Nucleoprotein; NA, neuraminidase; M, matrix protein; NS, nonstructural protein, tMRCA, inferred most recent common ancestor.

Appendix Table 5. Predicted N-glycosylation sites in HA proteins of avian influenza H5N2/Dominican Republic Strains

	Glycosylation site (H5 numbering)								
Strain/genetic cluster	27	39	142*	181*	252*	277	302	496	555
A/chicken/Dominican_Republic/07_002397_7/2007(H5N2)	NSTK	NVTV		NNTN	NDSI		NSSM	NGTY	NGSL
A/chicken/Dominican_Republic/17_041237_001/2017(H5N2) / A	NSTT	NVTV	NASA	NNTN			NSSM	NGTY	NGSL
A/chicken/Dominican_Republic/17_041237_004/2017(H5N2) / A	NSTT	NVTV	NASA	NNTN			NSSM	NGTY	NGSL
A/chicken/Dominican_Republic/19_020695_011_794_19_17/2019(H5N2) / A	NSTT	NVTV	NASA	NNTN			NSSM	NGTY	NGSL
A/chicken/Dominican_Republic/18_044726_013/2018(H5N2) / B	NSTK	NVTV	NASA	NNTN			NSSL	NGTY	NGSL
A/chicken/Dominican_Republic/17_035772_2/2017(H5N2) / B1	NSTK	NVTV	NATA	NNTN			NSSL	NGTY	
A/chicken/Dominican_Republic/17_035000_5/2017(H5N2) / B1	NSTK	NVTV	NATA	NNTN			NSSL	NGTY	
A/chicken/Dominican_Republic/17_035000_15/2017(H5N2) / B1	NSTK	NVTV	NATA	NNTN			NSSL	NGTY	
A/chicken/Dominican_Republic/17_035772_3/2017(H5N2) / B1	NSTK	NVTV	NATA	NNTN		NSTI	NSSL	NGTY	
A/chicken/Dominican_Republic/19_020695_010_729_19_2/2019(H5N2) / B2	NSTT	NVTV	NASA	NNTN	NDSI		NSSL	NGTY	NGSL
A/chicken/Dominican_Republic/19_020695_014_1590_19_7/2019(H5N2) / B2	NSTT	NVTV	NASA	NNTN	NDSI		NSSL	NGTY	NGSL
A/chicken/Dominican_Republic/19_020695_015_1590_19_8/2019(H5N2) / B2	NSTT	NVTV	NASA	NNTN	NDSI		NSSL	NGTY	NGSL
A/chicken/Dominican_Republic/19_020695_001_529_19_9/2019(H5N2) / B2	NSTT	NVTV	NASA	NNTD	NDSI		NSSL	NGTY	NGSL
A/chicken/Dominican_Republic/19_020695_005_705_19_10/2019(H5N2) / B2	NSTT	NVTV	NASA	NNTN	NDSI		NSSL	NGTY	NGSL
A/chicken/Dominican_Republic/19_020695_013_1136_19_11/2019(H5N2) / B2	NSTT	NVTV	NASA	NNTN	NDSI		NSSL	NGTY	NGSL
A/chicken/Dominican_Republic/19_020695_002_671_19_13/2019(H5N2) / B2	NSTT	NVTV	NASA	NNTD	NDSI		NSSL	NGTY	NGSL
A/chicken/Dominican_Republic/19_020695_003_671_19_14/2019(H5N2) / B2	NSTT	NVTV	NASA	NNTN	NDSI		NSSL	NGTY	NGSL
A/chicken/Dominican_Republic/19_020695_004_671_19_15/2019(H5N2) / B2	NSTT	NVTV	NASA	NNTN	NDSI		NSSL	NGTY	NGSL
A/chicken/Dominican_Republic/19_020695_012_1107_19_16/2019(H5N2) / B2	NSTT	NVTV	NASA		NDSI		NSSL	NGTY	NGSL

*Predicted N-glycosylation sites on antigenic site.

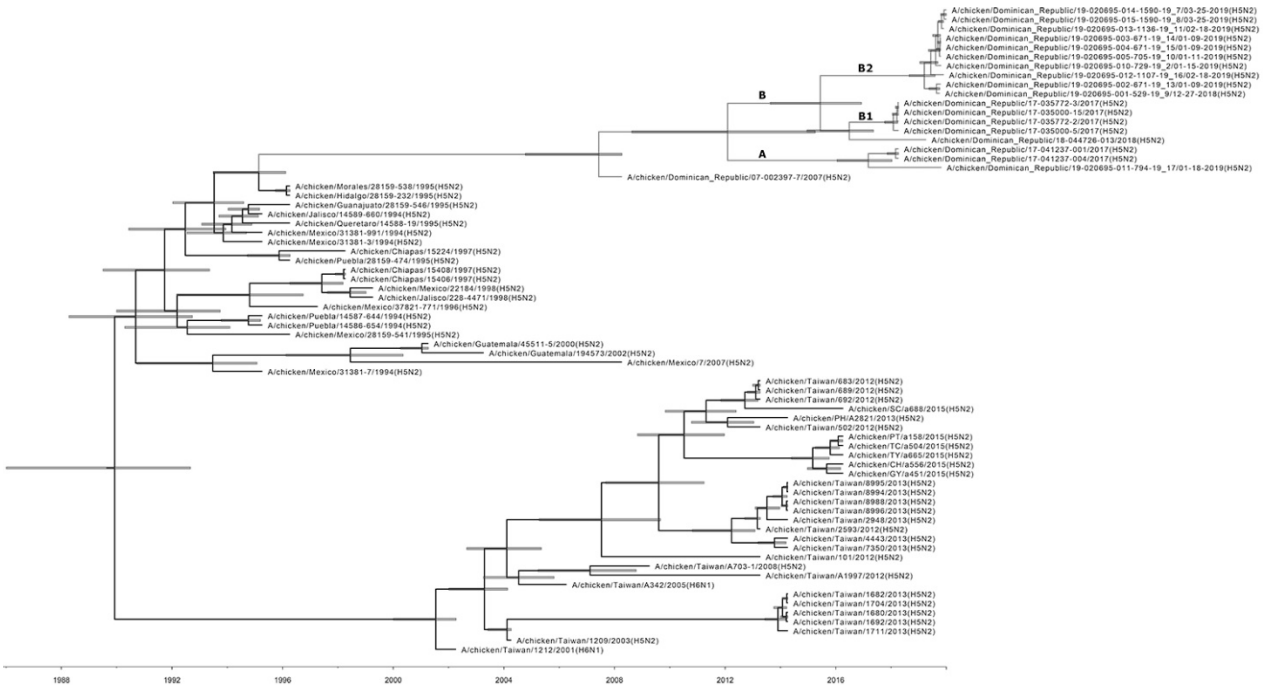

Appendix Figure 1. Maximum-likelihood phylogeny for the PB2 genome segment sequences of low pathogenicity avian influenza H5N2 viruses, Dominican Republic. Bootstrap values >70% are shown. The scale bar indicates the number of nucleotide substitutions per site.

Appendix Figure 2. Maximum-likelihood phylogeny for the PB1 genome segment sequences of low pathogenicity avian influenza H5N2 viruses, Dominican Republic. Bootstrap values >70% are shown. The scale bar indicates the number of nucleotide substitutions per site.

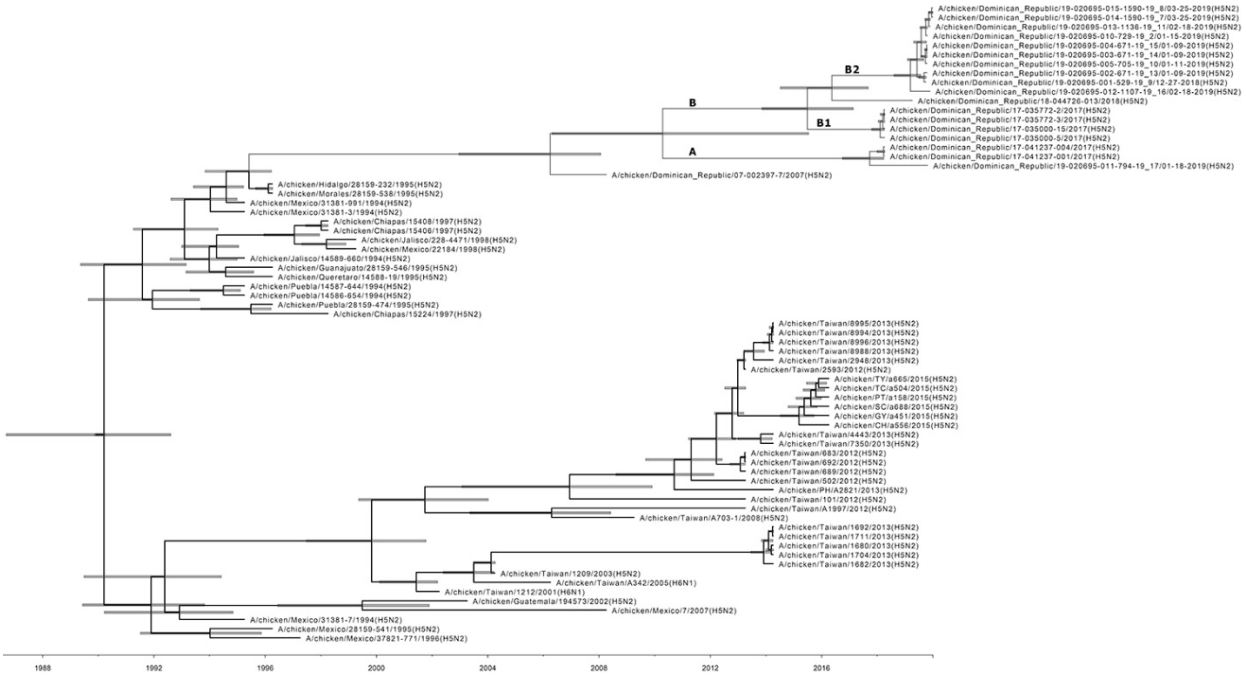

Appendix Figure 3. Maximum-likelihood phylogeny for the PA genome segment sequences of low pathogenicity avian influenza H5N2 viruses, Dominican Republic. Bootstrap values >70% are shown. The scale bar indicates the number of nucleotide substitutions per site.

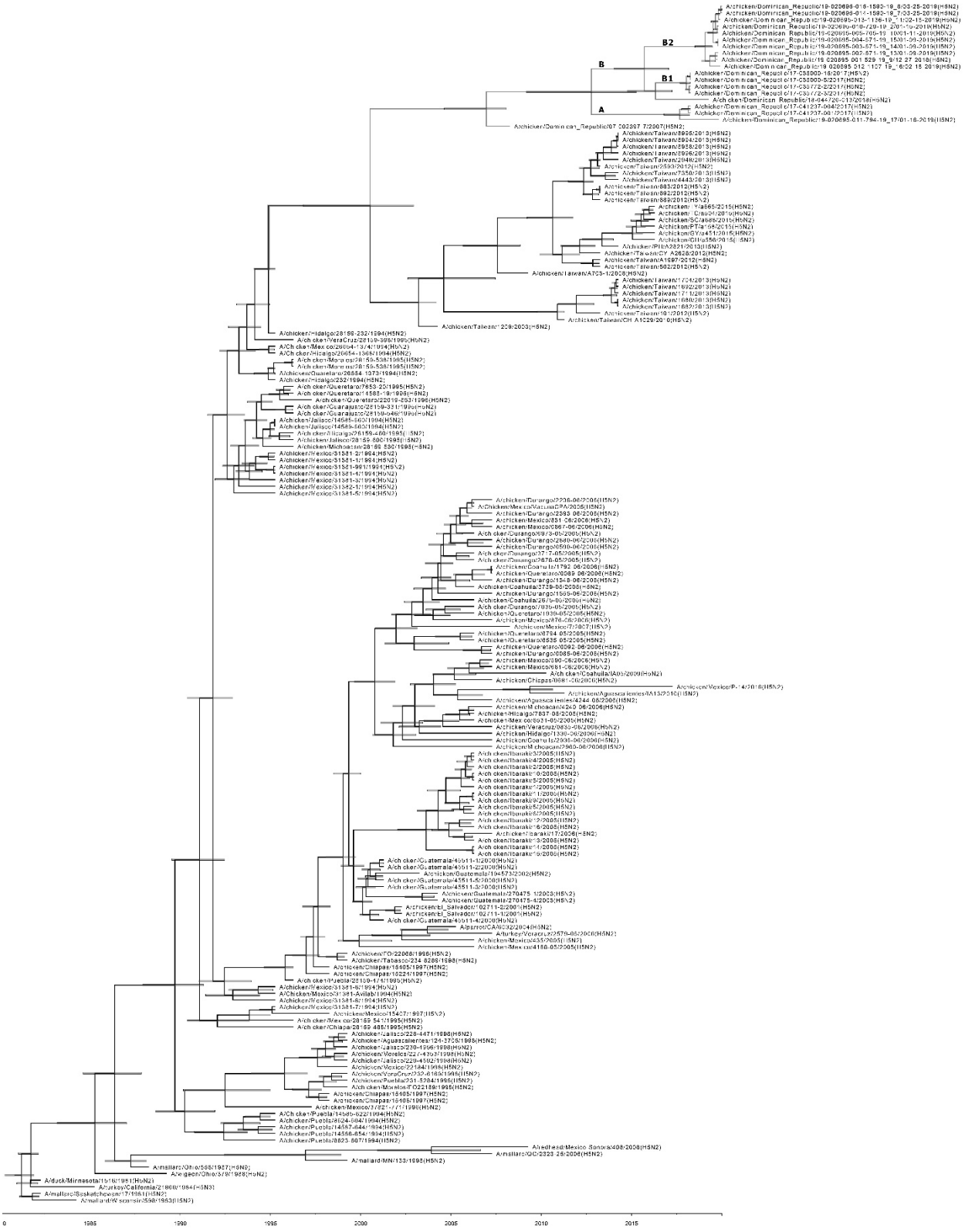

Appendix Figure 4. Maximum-likelihood phylogeny for the HA genome segment sequences of low pathogenicity avian influenza H5N2 viruses, Dominican Republic. Bootstrap values >70% are shown. The scale bar indicates the number of nucleotide substitutions per site.

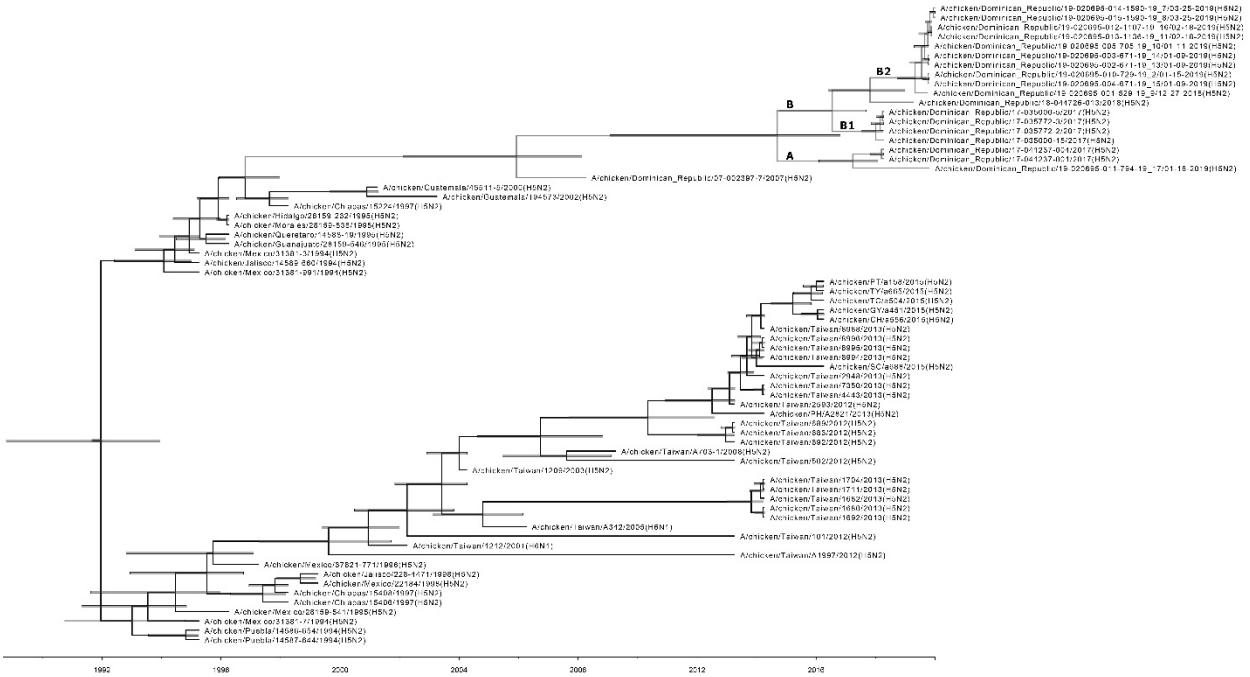

Appendix Figure 5. Maximum-likelihood phylogeny for the NP genome segment sequences of low pathogenicity avian influenza H5N2 viruses, Dominican Republic. Bootstrap values >70% are shown. The scale bar indicates the number of nucleotide substitutions per site.

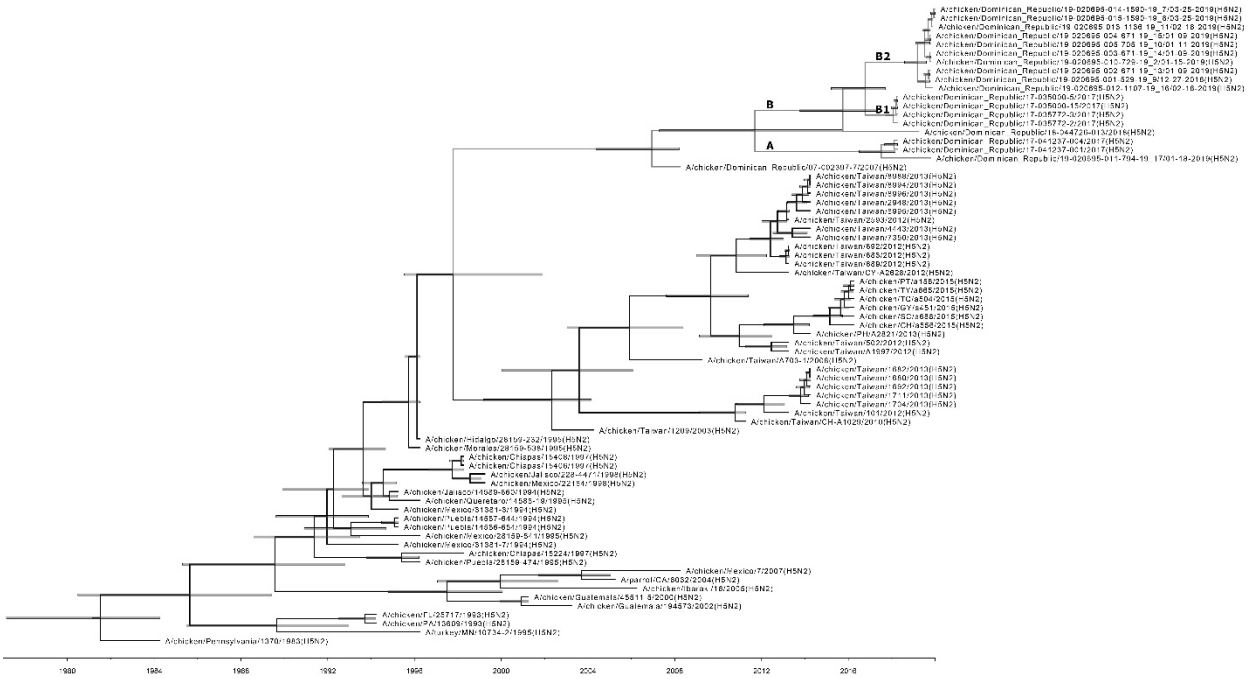

Appendix Figure 6. Maximum-likelihood phylogeny for the NA genome segment sequences of low pathogenicity avian influenza H5N2 viruses, Dominican Republic. Bootstrap values >70% are shown. The scale bar indicates the number of nucleotide substitutions per site.

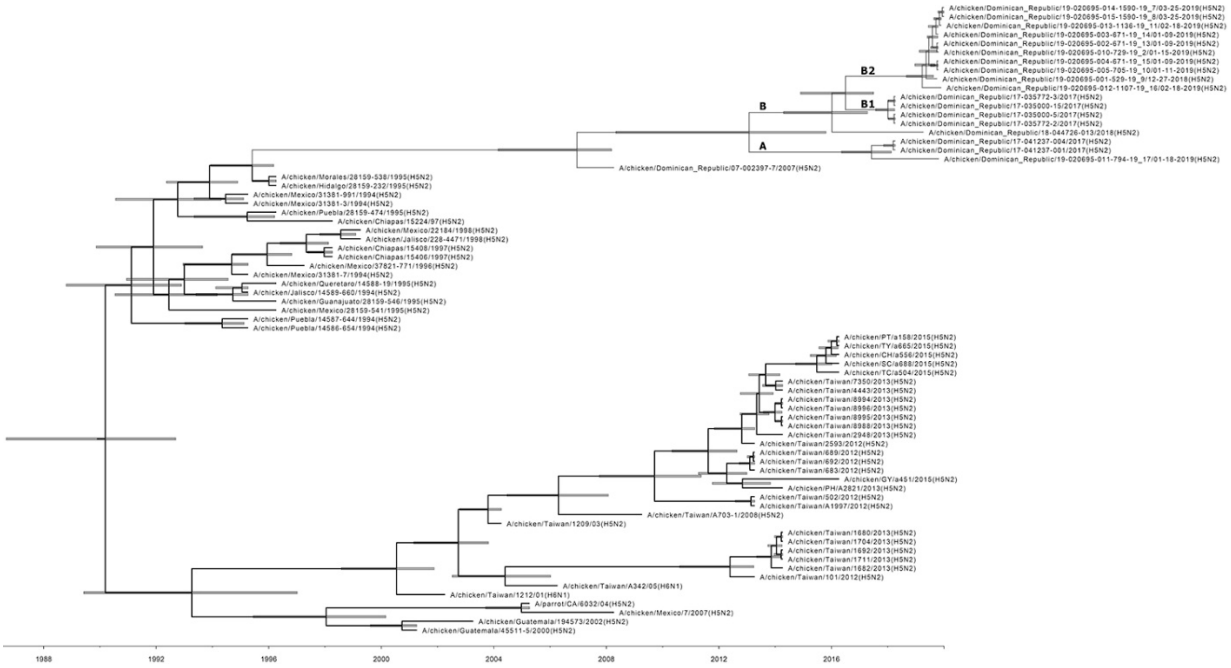

Appendix Figure 7. Maximum-likelihood phylogeny for the M genome segment sequences of low pathogenicity avian influenza H5N2 viruses, Dominican Republic. Bootstrap values >70% are shown. The scale bar indicates the number of nucleotide substitutions per site.

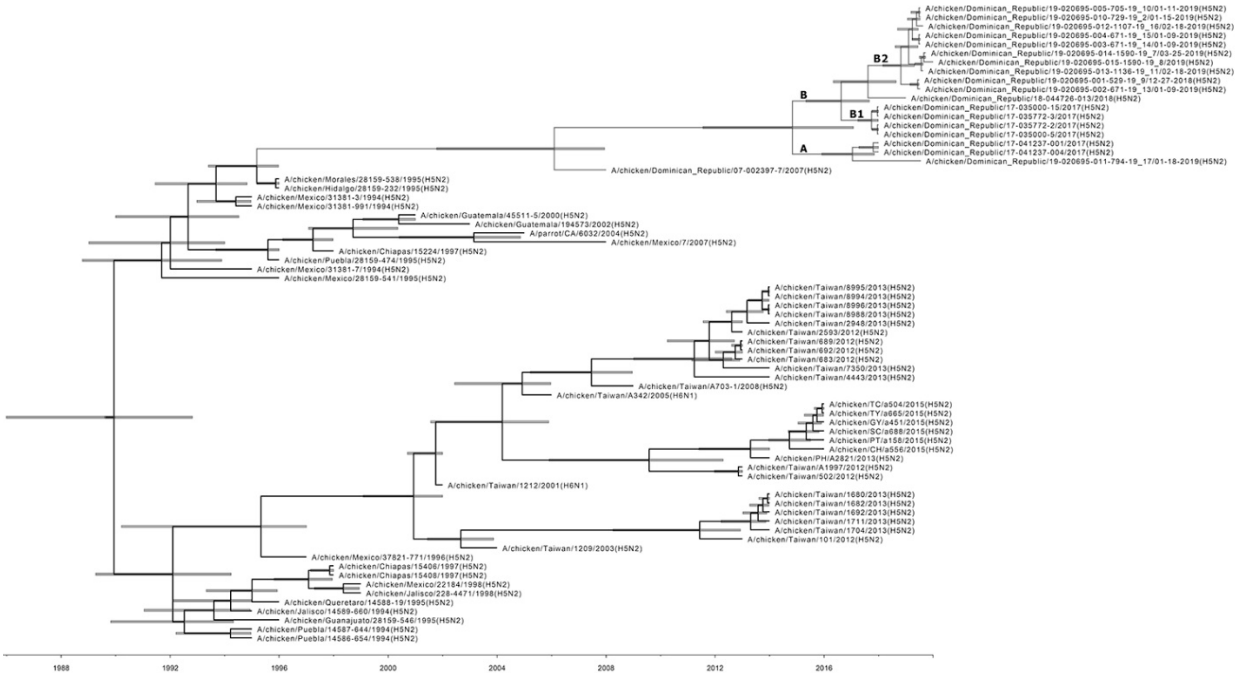

Appendix Figure 8. Maximum-likelihood phylogeny for the NS genome segment sequences of low pathogenicity avian influenza H5N2 viruses, Dominican Republic. Bootstrap values >70% are shown. The scale bar indicates the number of nucleotide substitutions per site.

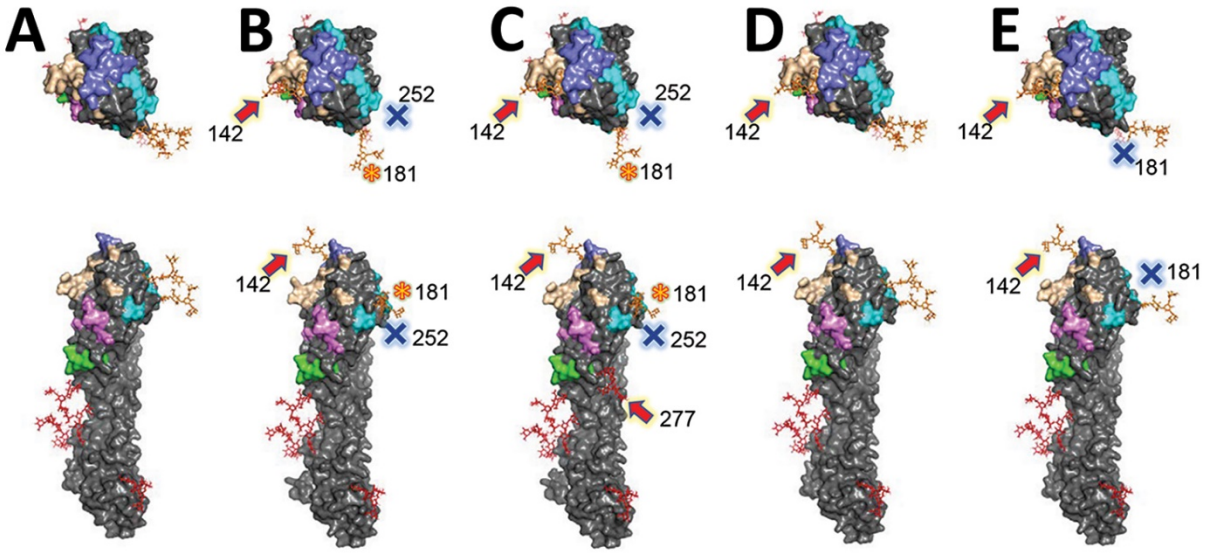

Appendix Figure 9. In silico 3-dimensional (3D) structure prediction and comparison of hemagglutinin protein of low pathogenicity avian influenza H5N2 virus, Dominican Republic. Only monomers are shown. A) CK/DR/07-002397-7/2007; B) genetic cluster A/B/B1 2017–2019; C) genetic cluster B1

CK/DR/035772-3/2017; D) genetic cluster B2, 2018–2019; E) genetic cluster B2 CK/DR/020695-012-1107/2019. Predicted antigenic sites are yellow-orange, slate, green, cyan, and violet. Predicted N-glycosylation sites located on antigenic sites are in orange and the others are represented with red. The N-glycosylation site patterns different from A/CK/Dominican_Republic/07–002397–7/2007 strain are indicated with red arrows for additions, blue crosses for deletions, and orange asterisks for predicted conformational change at antigenic–glycosylation site.